Am. Chem. Soc. 108, 8064-8068.
Wohlgemuth, R., Waespe-Sarcevic, N., & Seelig, J. (1980) Biochemistry 19, 3315-3321.
Yeagle, P. L. (1978) Acc. Chem. Res. 11, 321-327.
Yeagle, P. L., Hutton, W. C., & Martin, R. B. (1975) Proc. Natl. Acad. Sci. U.S.A. 72, 3477-3481.
Yeagle, P. L., Hutton, W. C., Huang, C., & Martin, R. B. (1976) Biochemistry 15, 2121-2124.
Yeagle, P. L., Hutton, W. C., Huang, C., & Martin, R. B. (1977) Biochemistry 16, 4344-4349.

Interaction of a Macrocyclic Bisacridine with DNA†

James M. Veal,‡ Ying Li,‡ Steven C. Zimmerman,§ Carol R. Lamberson,§ Michael Cory,∥ Gerald Zon,⊥ and W. David Wilson*,‡

Department of Chemistry, Georgia State University, Atlanta, Georgia 30303-3083, Department of Chemistry, University of Illinois, Urbana, Illinois 61801, Division of Organic Chemistry, Wellcome Research Laboratories, Burroughs Wellcome Co., Research Triangle Park, North Carolina 27709, and Applied Biosystems, Inc., 850 Lincoln Centre Drive, Foster City, CA 94404

Received May 14, 1990; Revised Manuscript Received August 28, 1990

ABSTRACT: The binding of the macrocycle SDM to DNA was investigated by visible spectroscopy, stopped-flow kinetics, and NMR spectroscopy. SDM is composed of two 9-aminoacridines linked via the amino groups by a spermine side chain and via the 4-positions by a *N,N'*-[(methylthio)ethyl]succinamide side chain [Zimmerman, S. C., Lamberson, C. R., Cory, M., & Fairley, T. A. (1989) *J. Am. Chem. Soc. 111*, 6805-6809]. The visible spectrum of SDM bound to poly[d(A-T)]$_2$ or poly[d(G-C)]$_2$ is red-shifted relative to the spectrum of SDM alone and displays considerable hypochromicity. Results from titrations of SDM with polymer indicate a binding site size of three base pairs per macrocycle. The dissociation constant for SDM bound to either poly[d(A-T)]$_2$ or poly[d(G-C)]$_2$ is an order of magnitude lower than that for a similar bisacridine linked only by a spermine side chain. In addition, the dependence of the dissociation constant on ionic strength is significantly reduced. NMR studies of SDM complexes with poly[d(A-T)]$_2$ or a tetramer, d(CGCG)$_2$, show that intercalation is the mode of binding. The magnitudes of the chemical shift differences for SDM aromatic protons in the free and bound states support intercalation with the acridine ring systems essentially parallel to the long axis of the base pairs. Cross peaks from NOESY spectra of the SDM complex with d(CGCG)$_2$ further support this mode of binding and provide information on the structure of the complex. The results are analyzed for consistency with each of three binding models: (i) bisintercalation with the two side chains in the same groove; (ii) bisintercalation according to the neighbor-exclusion principle with the two side chains in opposite grooves; and (iii) bisintercalation with two side chains in opposite grooves but with violation of the neighbor-exclusion principle. Model i is found to be unlikely on the basis of all evidence obtained, including preliminary modeling studies. Both models ii and iii can be reconciled with the experimental evidence and from a modeling standpoint are energetically feasible.

The classical view of DNA as a static B-form structure has been modified by high-resolution structural studies which have shown that the double helix geometry is sensitive to both local environment and DNA sequence (Saenger, 1984; Wells & Harvey, 1987; Blackburn & Gait, 1990). Similar studies of reversible DNA complexes with aromatic molecules have recently illustrated an even wider array of polymorphic behavior (Scott et al., 1988; Gao & Patel, 1989; Pelton & Wemmer, 1990; Wilson, 1990; Wilson & Li, 1990). The classical paradigms for intercalation and minor groove complexes are being substantially expanded by the discovery of interactions which show significant variations with ligand structure and DNA sequence.

Many unique interactions occur in DNA complexes with bisintercalators, and the development of additional bisintercalators and polyintercalators is of interest for several reasons. These compounds can bind to DNA with high affinity and be very specific in their base pair recognition (Wakelin, 1986; Laugaa et al., 1987; Hurley & Boyd, 1987; Gao & Patel, 1989). Some natural and synthetic bisintercalators have substantial anticancer activity (Wakelin, 1986; Delbarre et al., 1987; Hurley & Boyd, 1987; Jaycox et al., 1987; Gao & Patel, 1989). In addition, they can provide probes for large-amplitude DNA dynamics and may also serve as models for some types of protein-DNA interactions (Suzuki, 1990). In ways not possible for simple monointercalators, bisintercalators can induce substantial changes in DNA conformation and base pairing such as Watson-Crick to Hoogsteen base pairing in their complexes (Wakelin, 1986; Hurley & Boyd, 1987; Gao & Patel, 1988, 1989). Bisintercalators have also been reported to bind in violation of the phenomenological neighbor-exclusion principle (Atwell et al., 1985; Wakelin, 1986).

When the aromatic rings of bisintercalators are connected by more than one linking chain, they form macrocyclic systems which may bind to DNA by bisintercalation only if extensive base pair disruption occurs. The macrocyclic bisacridine SDM (Figure 1) has recently been designed and synthesized by Zimmerman et al. (1989). Preliminary physical studies using hydrodynamic, spectroscopic, and thermal-melting methods indicated that the macrocycle binds to DNA in a manner similar to a bisacridine connected by a single spermine chain, SPDA (Figure 1), which is an established bisintercalator

† W.D.W. acknowledges funding from the National Institutes of Health (NIH-NIAID AI-27196). S.C.Z. acknowledges funding from the National Science Foundation PYI Program (CHE-8858202).

* Corresponding author.
‡ Georgia State University.
§ University of Illinois.
∥ Burroughs Wellcome Co.
⊥ Applied Biosystems, Inc.

0006-2960/90/0429-10918$02.50/0 © 1990 American Chemical Society

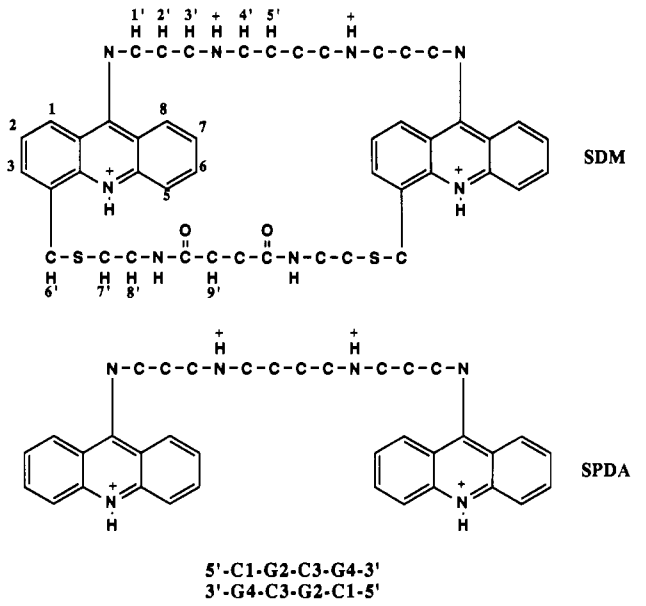

FIGURE 1: (Top) Chemical structure for the bisacridine macrocycle SDM, with the spermine linking chain at the top and the bisamide linking chain at the bottom. The proton numbering scheme is shown. (Middle) The spermine-linked bisintercalator SPDA. (Bottom) The base numbering scheme for the self-complementary $d(CGCG)_2$ duplex. Standard numbering for the base and deoxyribose protons is used (Wuthrich, 1986).

(Wright et al., 1980; Assa-Munt et al., 1985; Zimmerman et al., 1989). The linking chains on SDM are long enough to allow the molecule to bisintercalate according to the neighbor exclusion principle (Crothers, 1968). Such binding could occur with one linking chain in each of the DNA grooves or with both chains in the same groove. In addition to bisintercalation models which obey neighbor exclusion, less extended conformations of the macrocycle, which allow bisintercalation at adjacent sites in violation of the neighbor-exclusion model, are also possible. Such complexes could also have both chains in the same or in opposite grooves.

Kinetics studies of macrocycle–DNA reactions can help distinguish among models which require zero, one, or two base pairs to be disrupted in complex formation (dissociation). NMR[1] experiments on macrocycle–DNA complexes can help distinguish between conformations with both chains in the same groove or in opposite grooves. We report here visible spectral, kinetic, and NMR results for complexes of the macrocycle SDM with synthetic DNA polymers and with the tetramer $d(CGCG)_2$, as well as our analysis of the results in terms of the interaction models described above.

Materials and Methods

Visible Spectroscopy. Visible spectroscopy was performed by using a Cary 2200 spectrophotometer. MES buffer (10 mM MES, 1 mM EDTA, pH 6.5) containing 0.1 M NaCl was added to a 10-cm cuvette, and base-line spectra were recorded. Concentrated SDM (ϵ_{413nm} = 18000 M^{-1} cm^{-1}) was then added to the cuvette with a Hamilton syringe to a concentration of 5.5 μM, and absorption spectra were recorded from 500 to 320 nm. Small volumes of a solution of concentrated polymer DNA in MES buffer/0.1 M NaCl were then titrated into the SDM solution and the absorption spectrum rescanned after an incubation period of 4–15 min. The stock DNA polymer concentrations were determined by using an ϵ_{260nm} = 6600 M^{-1} cm^{-1} for poly[d(A-T)]$_2$ and ϵ_{254nm} = 8400 M^{-1} cm^{-1} for poly[d(G-C)]$_2$.

Kinetics. Kinetic measurements were conducted with a Hi-Tech SF-51 stopped-flow spectrometer. The software provided with the instrument was used for both data acquisition and analysis. The data acquisition was carried out via a high-speed (>80-kHz) 12-bit analog to digital convertor with a HP-330 computer interfaced to the SF-51 stopped-flow spectrometer. Single-wavelength kinetic records of voltage versus time were collected and converted to absorbance. Typically, several individual mixing experiments were collected and averaged by the computer to improve the signal to noise ratio. Dissociation reactions were monitored in a 10-mm path length cell in the stopped-flow spectrometer by mixing equal volumes (100 μL) of a DNA–drug complex solution with a 1% solution of SDS at the same salt concentration. The temperature was controlled by circulating water with a Haake A81 refrigerated water bath and was monitored with an internal thermistor in the SF-51 sample compartment.

NMR. The d(CGCG) oligonucleotide was synthesized, deblocked, and initially purified as previously described (Wilson et al., 1988). The oligonucleotide was then passed through a Chelex filter and further purified by chromatography using a Vydak C-18 reverse-phase column/Rainin Rabbit HPLC system interfaced to an Apple Macintosh SE computer. The DNA was collected and quantified by using an extinction coefficient of 8675 M^{-1} cm^{-1} (Warshaw & Cantor, 1970). The $d(CGCG)_2$ duplex was then formed by dissolving the oligonucleotide in deuterated acetate–EDTA buffer (45 mM CD_3COOD/20 μM EDTA/pD to 5.5 with NaOH in 99.8% D_2O). The solution was then filtered through a Millipore nylon 66 filter.

The SDM macrocycle was dissolved to a stock concentration of 5 mM in D_2O. The drug–DNA complex was then prepared by adding the concentrated SDM to a 2.5 mM $d(CGCG)_2$ duplex solution in acetate–EDTA buffer. Addition was in small increments via a Hamilton 10-μL syringe under gentle stirring to a calculated concentration of 1 mM SDM. As was repeatedly observed for other attempted preparations of the complex, significant precipitation occurred. The sample was then clarified by centrifugation, twice dried by streaming N_2, and redissolved in 99.96% D_2O. The final concentrations were approximately 0.6 mM SDM and 2.0 mM CGCG duplex.

^{1}H NMR 1D and 2D (phase-sensitive NOESY and COSY) experiments were performed at 25 and 40 °C on a Varian VXR400 spectrometer (States et al., 1982). At 25 °C side-chain motion was reduced although the SDM aromatic resonances were severely broadened. A temperature of 40 °C was chosen because broadening of the aromatic SDM resonances was significantly reduced while a well-formed duplex was maintained. For the NOESY and COSY experiments, 1K complex points were recorded for each of 256 t_1 increments over a spectral width of 4000 Hz. A 1.5-s delay time between scans and a mixing time of 400 ms were typically used for the NOESY experiments. The HDO signal was reduced by selective irradiation during the delay time. Due to the low complex concentration, 256 scans were acquired per t_1 increment. The data were transferred to a Silicon Graphics Iris workstation and processed by using Hare Research Inc. FTNMR software. The data were weighted and apodized by a sine bell squared function phase-shifted 60–90° and zero-filled to 2K in both dimensions prior to Fourier transformation. The spectrum for the first t_1 value was also multiplied by 0.5 prior

[1] Abbreviations: NMR, nuclear magnetic resonance; COSY, two-dimensional autocorrelated spectroscopy; NOESY, two-dimensional nuclear Overhauser spectroscopy; MES, 2-(*N*-morpholino)ethanesulfonic acid; EDTA, ethylenediaminetetraacetic acid; SDS, sodium dodecyl sulfate; TMS, tetramethylsilane.

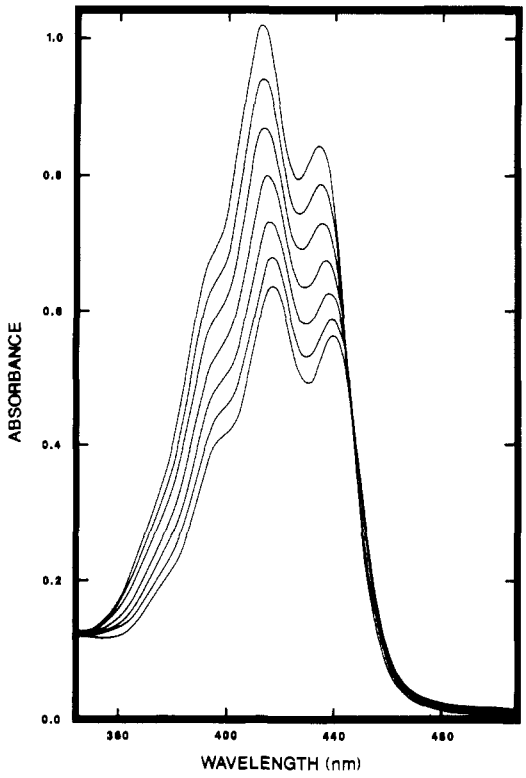

FIGURE 2: A visible absorption spectral titration of SDM with poly[d(A-T)]$_2$ in MES buffer with 0.1 M NaCl at 25 °C.

to Fourier transformation to minimize t_1 noise (Otting et al., 1986). DNA and SDM chemical shifts were referenced to the HDO resonance (prior to decoupling) whose chemical shift had previously been determined relative to TMS.

Molecular Modeling. Molecular mechanics models of SDM were generated by using MacroModel version 3.0 (Mohamadi et al., 1990), the AMBER force field (Weiner et al., 1986), and methods previously developed for DNA intercalating agents (Besterman et al., 1989). Double-stranded hexa- or undecanucleotide sequences with central CGCG base pairs were generated in standard B-DNA geometry (Arnott & Hukins, 1972), and intercalation sites (neighbor excluded and non neighbor excluded) were developed by employing geometric constraints on inter-ring distances, base pair hydrogen bonds, and backbone torsion angles. The SDM molecule was modeled with a formal charge of 4+ by using the nitrogen of the acridines fully charged. Atomic charges on SDM were generated by the MacroModel program from bond dipole parameters. Geometric constraints were used to develop specific neighbor-excluded and non-neighbor-excluded SDM conformations. Minimizations were performed by using the block diagonal Newton Rafeson (BDNR) minimization technique with a distance-dependent dielectric constant, $\epsilon = r_{ij}$. Constraints forcing macrocycle inter-ring distances were set to generate models with an acridine ring separation of 10.2 or 6.8 Å in partially minimized models. After partial minimization of the constrained molecule, the constraints were removed and each model was fully minimized.

RESULTS

Absorption Spectra. SDM has a classical acridine visible absorption spectrum (Figure 2) and obeys Beer's law up to a concentration of at least 1×10^{-5} M in MES buffer with 0.1 M NaCl. Titration of the compound with poly[d(A-T)]$_2$ in the same buffer results in a pronounced hypochromicity and slight shifts of the acridine absorption peaks to longer wavelengths (Figure 2). Isosbestic points at 446 and 350 nm in-

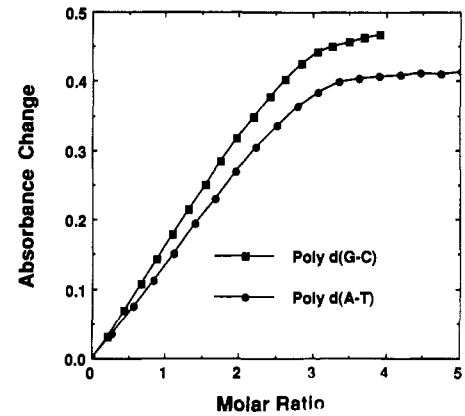

FIGURE 3: Absorbance change at 413 nm versus the molar ratio of polymer base pairs to SDM for titration of SDM with poly[d(A-T)]$_2$ and poly[d(G-C)]$_2$. The experiments were conducted as described in Figure 2.

dicate a single observable mode of binding of SDM to DNA. Very similar spectral titration curves are obtained on titrating SDM with poly[d(G-C)]$_2$ (not shown). Identical absorption spectra were observed for a given concentration of DNA following incubation periods of 4 and 15 min, indicating that no detectable very slow association step was present. The absorbance changes at the free SDM maximum absorption wavelength (413 nm) are plotted in Figure 3 for the polymer titrations as a function of the ratio of moles of polymer base pairs to moles of macrocycle. As can be seen, there is a slightly greater hypochromicity in the titration with poly[d(G-C)]$_2$ than with poly[d(A-T)]$_2$, but both titration curves have a break point at a ratio of approximately three base pairs per macrocycle. This result indicates that each macrocycle binding site requires three base pairs in complexes with both poly[d(A-T)]$_2$ and poly[d(G-C)]$_2$. Titrations of SPDA with the DNA polymers were also attempted, but isosbestic points were not obtained. Dimerization and/or multiple DNA binding modes may occur with the structurally simpler and more flexible bisacridine.

Dissociation Kinetics. The changes in macrocycle absorbance on complex formation or dissociation can also be used to follow the kinetics of the reactions with DNA. Sequestering of free drug by anionic SDS micelles is an efficient method for driving the dissociation reaction without perturbing the anionic DNA molecule. Studies with a wide range of DNA binding compounds including acridines (Wakelin et al., 1987), actinomycins (Muller & Caruthers, 1968), porphyrins (Strickland et al., 1988), and anthraquinones (Denny & Wakelin, 1990) have shown that the dissociation rate is not influenced by the presence of SDS. Transferring the organic ligands from the DNA complex to the SDS phase generally results in minimum solubility problems and in spectral changes that are not complicated by self-aggregation.

An absorbance versus time curve for the SDS-driven dissociation reaction of a complex of the bisacridine macrocycle with poly[d(G-C)]$_2$ is shown in Figure 4A. The results are reasonably well fitted with a single exponential curve although there is an improvement in both the rms deviation and in the residual plot after adding a small amount (~20% of the total amplitude) of a second exponential (Table I). A similar dissociation experiment is shown in Figure 4B for the bisacridine SPDA which has a single linking chain. The dissociation rate constant for the SPDA complex under these conditions is ~10 times faster than with SDM. In addition, the dissociation reaction of SPDA clearly requires two exponential curves for adequate fitting. The rate constants for the

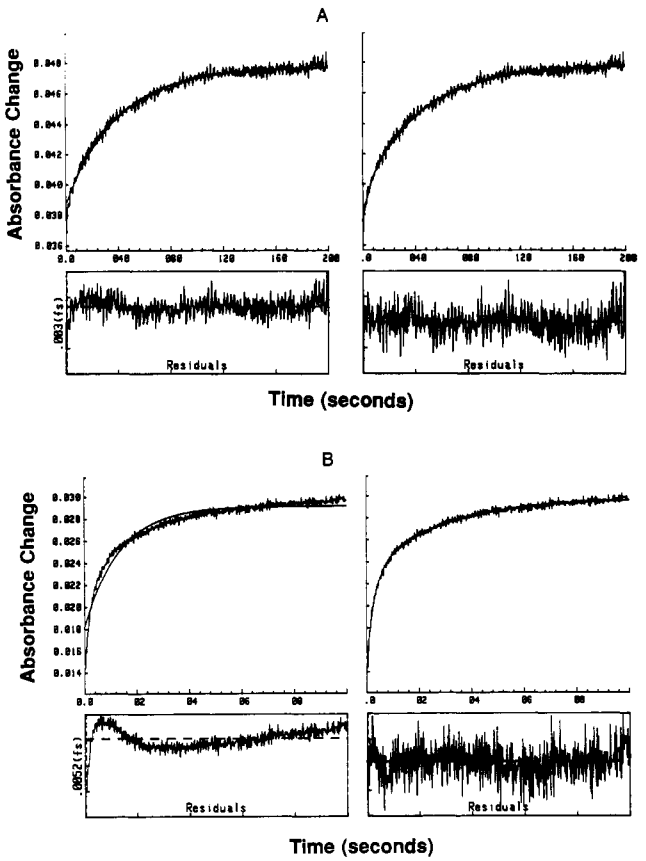

FIGURE 4: Absorbance versus time plots for the SDS-driven dissociation of (A) the SDM–poly[d(G-C)]$_2$ complex and (B) the SPDA–poly[d(G-C)]$_2$ complex. The left and right panels show the fits obtained by using single- and double-exponential curves, respectively (residual absorbance at bottom).

Table I: Dissociation Kinetics Results for Complexes of SDM, SPDA, and Nogalamycin with Poly[d(A-T)]$_2$ and Poly[d(G-C)]$_2$[a]

compound	k (s^{-1})	k_1	% A_1	k_2	% A_2	k_{app} (s^{-1})
		Poly[d(A-T)]$_2$				
SDM	0.15	0.16	87	0.03	13	0.14
SPDA	0.79	2.5	32	0.63	68	1.2
nogalamycin	0.05					
		Poly[d(G-C)]$_2$				
SDM	0.026	0.19	18	0.023	82	0.055
SPDA	0.67	2.9	56	0.29	44	1.8
nogalamycin	0.00024					

[a] Conditions for SDM and SPDA values are 30 °C in MES buffer and 0.10 M NaCl. Conditions for nogalamycin values are 40 °C in MES buffer and 0.01 M NaCl (Fox et al., 1985).

two exponential processes differ by a factor of ~10 and have similar amplitudes (Table I). Because the dissociation curves have no fine structure, the amplitudes and rate constants in the two exponential fits are highly correlated and this can lead to some base-line and noise level dependence in fitting individual curves which have similar shapes and apparent half-lives. To improve the direct comparisons between results for dissociation of the two bisacridines, an apparent complex lifetime (τ), characterizing the entire dissociation reaction, was calculated:

$$\tau = 1/k_{app} = 1/(A_1k_1 + A_2k_2) \quad (1)$$

where the A and k values refer to amplitudes and rate constants, respectively, from the two exponential curves in the fitting. The τ values are much less sensitive to small differences in base line and noise level, and there is little variation in calculated τ values among individual dissociation experiments conducted under the same experimental conditions. Comparisons of τ and/or k_{app} values can, thus, be made with high precision. All values for the dissociation kinetics for the complexes of the two bisacridines with poly[d(G-C)]$_2$ are collected in Table I.

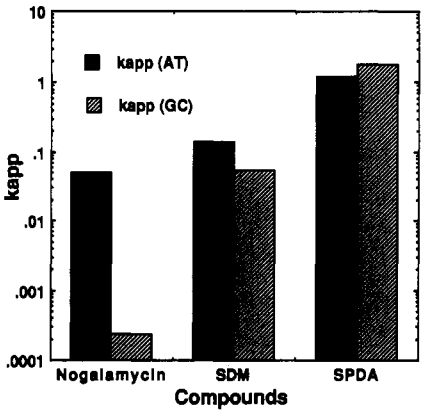

FIGURE 5: A histogram for the comparison of SDS-driven dissociation rate constants for poly[d(A-T)]$_2$ and poly[d(G-C)]$_2$ complexes of SDM and SPDA (at 30 °C and 0.12 M [Na^+]) and nogalamycin (at 40 °C and 0.01 M [Na^+]). The nogalamycin results are from Fox et al. (1985).

Similar SDS-driven dissociation experiments were performed with complexes of SDM and SPDA with poly[d(A-T)]$_2$ (Table I). As with poly[d(G-C)]$_2$, the SDM results were well fitted with a single exponential curve but were improved with the addition of a small amount (~10% of the total amplitude) of a second exponential. The SPDA–poly[d(A-T)]$_2$ results clearly require a two-exponential fit as with the poly[d(G-C)]$_2$ complex of this compound (Table I). Results for the SDS-driven dissociation of nogalamycin, an anthracycline derivative with bulky substituents which requires disruption of DNA base pairs for dissociation, from poly[d(G-C)]$_2$ and poly[d(A-T)]$_2$ complexes are also included in Table I for comparison (Fox et al., 1985). A histogram (Figure 5) and Table I summarize the results from these experiments and illustrate the following points. The dissociation rate constants of SDM from poly[d(G-C)]$_2$ and poly[d(A-T)]$_2$ are an order of magnitude smaller than those for SPDA. The dissociation rate constant of SDM from poly[d(A-T)]$_2$ is approximately 5 times larger than that from poly[d(G-C)]$_2$, whereas the dissociation rate constants of SPDA from poly[d(G-C)]$_2$ and poly[d(A-T)]$_2$ are nearly equal. The nogalamycin and SDM dissociation rate constants are similar for their poly[d(A-T)]$_2$ complexes, but very different for their poly[d(G-C)]$_2$ complexes, with the nogalamycin value being much smaller.

In an effort to determine if the SDM dissociation reactions contain a very slow dissociation phase that is not easily observed in the limited time periods of the stopped-flow experiments (~400 s), the reactions were also conducted in a split compartment cell on a Cary 219 spectrophotometer. After collection of a base line, the reaction was initiated with hand mixing and the absorbance was monitored for several hours. Over 80% of the dissociation reaction of SDM from poly[d(A-T)]$_2$ occurred during mixing, and no slow change in absorbance could be detected. A somewhat larger percentage of the dissociation reaction with poly[d(G-C)]$_2$ could be detected; however, as with the poly[d(A-T)]$_2$ complex, no long-term absorbance change could be detected. The rate constants estimated from the hand-mixing experiments agree quite well with the higher resolution results from the stopped-flow experiments described above. To determine whether a different type of complex could be formed very slowly, SDM

Table II: Chemical Shifts (δ in ppm) and Chemical Shift Differences ($\Delta\delta$, Free – Bound) for SDM in the Absence and Presence of $d(CGCG)_2$[a]

resonance	δ_{free}	δ_{bound}	$\Delta\delta$
SDM 1	8.19	7.45	0.74
2	7.45	6.60	0.84
3	7.77	7.23	0.54
5	7.86	7.38	0.48
6	7.78	7.07	0.71
7	7.41	6.74	0.67
8	8.15	7.68	0.47
SDM 1′	4.14	3.84	0.30
2′	2.30	2.21	0.09
3′	3.15	3.19	−0.04
4′	3.03	3.13	−0.10
5′	1.72	1.85	−0.13
6′	4.14	3.84	0.30
7′	2.56	2.62	−0.06
8′	3.15	3.42	−0.27
9′	2.10	2.51	−0.41

[a] Chemical shifts for SDM free are in D_2O. Chemical shifts for SDM in its complex with $d(CGCG)_2$ are in acetate–EDTA buffer.

was heated with poly[d(A-T)]$_2$ at 60 °C for 8 h [the T_m of the SDM–poly[d(A-T)]$_2$ complex is over 80 °C]. The stopped-flow dissociation experiment was then repeated with the SDM–poly[d(A-T)]$_2$ complex, and the results were identical within experimental error with those obtained for an unheated sample. Thus, there does not appear to be any significant amount of an SDM–DNA complex which forms and dissociates more slowly than those described by the results in Table I.

Increasing salt concentration results in increased dissociation rate constants for complexes of cationic ligands with DNA (Manning, 1978; Record et al., 1978; Wilson et al., 1985). Dissociation of SDM and SPDA complexes with poly[d(A-T)]$_2$ was monitored over a range of salt concentrations, and the results are plotted as log k_{app} versus log [Na^+] in Figure 6 (see supplementary material). As expected, dissociation rate constants for both complexes increase with increasing salt concentration. A significant difference in slope is observed for the two complexes, with the slope of the SDM complex (1.6) reduced by $\sim 1/2$ that of the SPDA complex (2.8). This difference in slope is unusual since intercalators with the same charge are generally expected to have the same slope in plots such as those shown in Figure 6 (supplementary material).

NMR. To obtain additional information on the macrocycle–DNA complex, NMR studies were initiated with oligonucleotides (at the millimolar concentration level). Extensive precipitation occurred during sample preparation with several oligomer sequences, perhaps reflecting a complex aggregation induced by the spermine side chain and the overall 4+ charge of the macrocycle. Other similar bisacridine macrocycles, which lack the spermine side chain and have overall charges of 2+, form relatively soluble complexes with DNA. SDM alone is soluble in NaH_2PO_4 buffer but poorly soluble in Na_2HPO_4 buffer. Critical factors for improving the solubility are, consequently, a short oligomer sequence [d(CGCG)] and a high oligomer to SDM ratio. The excess DNA serves a "chain termination" function by limiting the extent of complex aggregation. Acetate buffer and low pD also appear to improve the solubility. Even with these solubility difficulties, the SDM complex was chosen for detailed NMR analysis because the complex is stable to quite high temperature (>40 °C) and gives relatively sharp, resolved spectral lines.

The 1D NMR spectra at 40 °C of SDM in D_2O and the SDM–$d(CGCG)_2$ complex in acetate–EDTA buffer are shown in Figure 7, and the chemical shifts are summarized in Table II. Chemical shifts for the CGCG duplex protons in the absence and presence of SDM are assigned according to standard 2D NMR procedures (Wuthrich, 1986), and the assignments for the free duplex are in agreement with those previously reported (Cheng et al., 1984; Delbarre et al., 1987). SDM and CGCG protons in the complex give single signals at 40 °C which are broadened relative to those in the free state. In the complex the duplex resonances are all (except C1 5′/5″) shifted upfield relative to the free state. The magnitudes of the shifts are largest for the H1′ and H5 protons (0.1–0.2 ppm). Given the fast exchange and an approximately 1:3 ratio of bound duplex to free duplex, the bound $d(CGCG)_2$ protons would then be shifted upfield approximately 0.3–0.6 ppm relative to the free state.

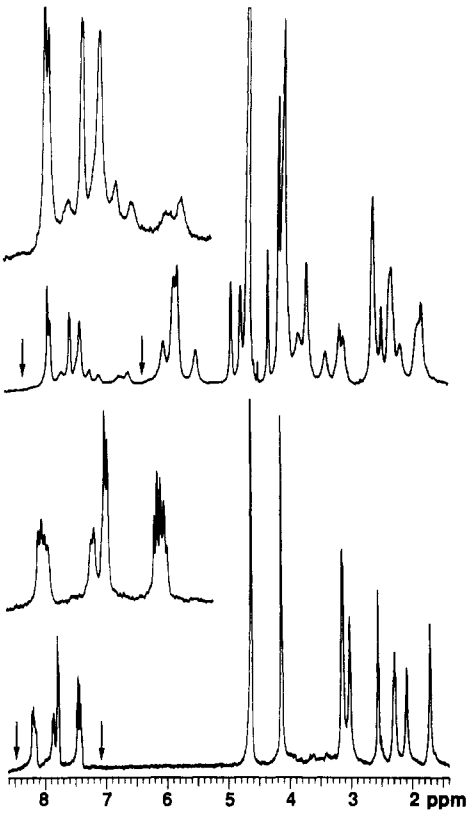

FIGURE 7: 1D ^1H NMR spectrum of (bottom) the SDM macrocycle in D_2O at 40 °C and (top) the SDM–$d(CGCG)_2$ complex in acetate–EDTA buffer at 40 °C. The arrows indicate the regions of the spectra expanded in the insets.

The free and bound SDM resonances are also assigned from NOESY and COSY spectra. The same strategy is used to assign the drug resonances for both free and complexed SDM (Figures 8 and 9). Initially, SDM 2′ is assigned on the basis of its two strong cross peaks—to SDM 1′ and 3′—which are then distinguished on the basis of the significant cross peaks between SDM 1′ and the SDM aromatic protons (Figure 9). SDM 6′ is also assigned on the basis of its cross peak to the aromatic proton SDM 3 (Figure 9). SDM 7′ and 8′ are assigned from cross peaks to SDM 6′. SDM 4′ and 5′ are then distinguished from 9′ on the basis of their cross peak to each other and specifically assigned from a weaker cross peak between SDM 4′ and 2′. The two sides of the acridine ring system (1–2–3 and 5–6–7–8) show the expected one-two-one and one-two-two-one sets of cross peaks (Figure 8). SDM 1 is distinguished from SDM 3 on the basis of its additional cross peak to SDM 2′ (as SDM 1′ and SDM 6′ are overlapped). Similarly, SDM 8 is distinguished from SDM 5 on the basis of an additional cross peak from SDM 8 to SDM 2′ (Figure 9), thereby distinguishing SDM 6 from SDM 7. All assign-

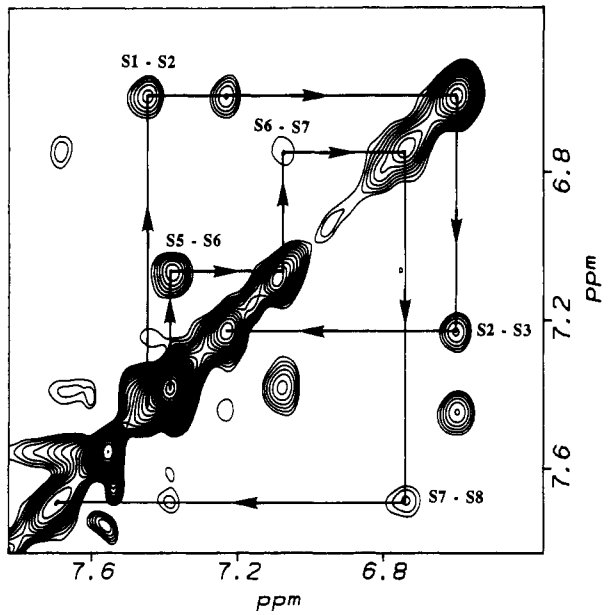

FIGURE 8: Expanded aromatic region of NOESY spectral contour plot showing SDM to SDM cross peaks in the SDM–d(CGCG) complex.

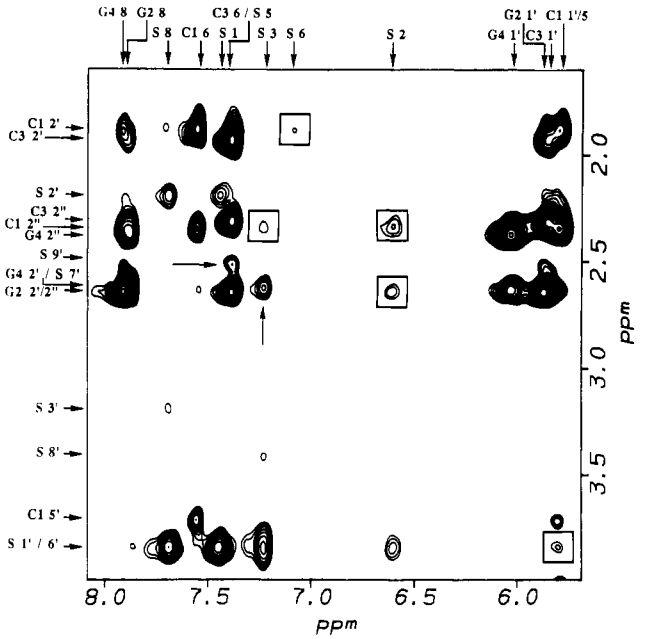

FIGURE 9: Expanded region of NOESY spectral contour plot. The squares enclose SDM to d(CGCG)$_2$ cross peaks, and the arrows denote SDM to SDM cross peaks between protons widely separated in covalent structure.

ments of resonances for SDM are consistent with the observed splitting patterns for individual protons and with COSY results.

The aromatic resonances of SDM bound to the d(CGCG) duplex are all shifted significantly upfield relative to those observed for unbound SDM in solution (Table II). The magnitudes of the shifts, 0.5–0.9 ppm, are indicative of intercalative binding (Wilson & Li, 1991). The largest shift is exhibited by SDM 2 followed by SDM 1, 6, and 7, and the smallest shifts are exhibited by SDM 3, 5, and 8. The chemical shifts of the amide and spermine side-chain protons are characterized by a common pattern with respect to distance from the acridine ring systems. The two protons closest to the acridines, SDM 1′ (spermine linker) and 6′ (amide linker), exhibit nearly identical upfield chemical shifts (0.30 ppm). The next adjacent protons, SDM 2′, 3′, and 7′, are nearly

Table III: SDM Intramolecular Cross Peaks Observed in the SDM–d(CGCG)$_2$ Complex[a]

	1	2	3	5	6	7	8		
SDM 8						S	/	/	SDM 9′
7					S	/	/	W	8′
6				S	/	/	S		7′
5				/	/	M	M		6′
3		S	/	/					5′
2	S	/	/	S					4′
1	/	/		W					3′
	/	S	W						2′
	S	S							1′
SDM 1′	2′	3′	4′	5′	6′	7′	8′	9′	

	1′	2′	3′	4′	5′	6′	7′	8′	9′
SDM 1	S	M	W						
2						W			
3						S	M	W	
5									M
8	S	M	W						

[a] Top: Aromatic to aromatic (above the diagonal) and aliphatic to aliphatic (below the diagonal) cross peaks. Bottom: Aromatic to aliphatic cross peaks. S, strong; M, moderate, W, weak.

unchanged with regard to chemical shift in the absence or presence of the duplex. All of the other side-chain resonances are shifted downfield by greater than 0.1 ppm in the bound vs free states. SDM 8′ and 9′, which flank the amide group, are the most downfield shifted (−0.27 and −0.41 ppm).

Two additional drug–drug cross peaks occur between protons widely separated in the covalent structure (Table III and Figure 9). They are SDM 9′ to 5 and SDM 7′ to 3. These aromatic to side chain cross peaks, which are significant in intensity, limit the extension possible for the amide side chain. In addition, they cannot both be accommodated by one structure and, consequently, require the two halves of the amide side chain to be in different conformations, thereby yielding an asymmetric structure for the bound SDM molecule. In addition to the observed drug–drug cross peaks, there is notably an absence of any cross peaks between protons of the two linker chains.

Analyses of NOESY cross peaks between SDM and the CGCG duplex were complicated by three factors: (i) the overall concentration and signal intensity of the sample was low; (ii) the excess d(CGCG)$_2$ present resulted in stronger intensities of duplex to duplex cross peaks and partially obscured potential duplex to SDM cross peaks in regions of spectral overlap; and (iii) several key resonances have nearly identical chemical shifts, particularly SDM 1′/6′ and C1 1′/5. Some resolution of the C1 1′/5 protons was obtained in the 25 °C NOESY spectra although all SDM protons are significantly broadened at this temperature.

The observed SDM to d(CGCG)$_2$ cross peaks at 40 °C are primarily between the aromatic protons of SDM and the H1′, H2′, and H2″ protons of the DNA. The most intense cross peaks are SDM 2 to C1 2″ and SDM 3 to C1 2″ (Figure 9 and Table IV), indicating close contact between these protons of the acridine ring systems and the duplex. Other SDM to d(CGCG)$_2$ cross peaks that are classified as strong are SDM 6 to C1 2′ and SDM 1′/6′ to C1 1′/5. The NOESY spectra at 25 °C further limit the latter cross peak to C1 5 to either SDM 1′ or 6′. Moderate intensity cross peaks are SDM 2 to G2 2″, SDM 3 to C3 1′, SDM 6 and 7 to C1 2″, SDM 6 to C1 1′/5, and SDM 1′/6′ to C3 1′. The SDM 3 to C3 1′ places the amide side chain in the minor groove of the duplex. Less definitive cross peaks are SDM 2 to C3 2′, SDM 9′ to C3 1′ or G2 1′, and SDM 2′ to G2 8. The SDM 9′ to C3 1′ or G2 1′ cross peak again places the amide side chain in the minor

Table IV: Summary of SDM to $d(CGCG)_2$ Cross Peaks[a]

	SDM 2	3	6	7	8	1′/6′	2′	9′
C1 1′/5			M			S		
C1 2′			S		W			
C1 2″	S	S	M	M				
G2 2″	M							
G2 8							W	
G3 1′		M				M		W
C3 2′								
5′/5″	W	W			W			W

[a] Intensities are as follows: S, strong; M, moderate; W, weak (intensity scale is not the same as used to evaluate the intramolecular SDM cross peaks in Table III).

Scheme I: Cartoon Models for SDM (Hatched) Binding to a DNA Tetramer Duplex (Solid)[a]

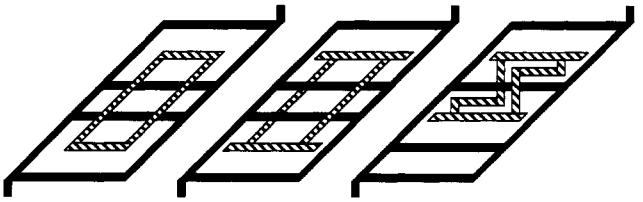

[a] (Left, model i) Bisintercalation according to the neighbor-exclusion principle with the SDM side chains in the same groove. (Middle, model ii) Bisintercalation according to the neighbor-exclusion principle with the SDM side chains in opposite grooves. (Right, model iii) Bisintercalation in violation of the neighbor-exclusion principle with the SDM side chains in opposite grooves.

groove, and the SDM 2′ and G2 8 cross peak places the spermine side chain in the major groove of the duplex. SDM 2, 3, 8, and 9′ also show apparent weak cross peaks to the DNA 5′/5″ region of the spectra.

Discussion

Binding Models. Previous hydrodynamic and thermal stability results (Zimmerman et al., 1989) along with the kinetics and NMR results presented here strongly support a bisintercalation binding model for SDM. Bisintercalation of the macrocycle (Scheme I) can occur through formation of three types of complexes: (i) a bayonet model with both side chains in the same groove and with the long axes of the acridine approximately perpendicular to the long axes of the base pairs at the binding site; (ii) a full intercalation model with the long axes of the acridines approximately parallel to the long axes of the base pairs and the acridines forming a two base pair sandwich in accordance with the neighbor-exclusion principle; or (iii) a second full intercalation model with the acridines bound at adjacent sites in violation of neighbor exclusion. The latter two models both require the spermine and amide side chains to be in opposite grooves and, consequently, necessitate temporary disruption of the DNA base pair hydrogen bonds for complex formation.

Absorbance Spectra. Significant hypochromicity and a red-shifted absorbance maximum upon addition of DNA to a solution of SDM were consistent with bisintercalation as the mode of binding. Because of the strong DNA–SDM interaction (Zimmerman et al., 1989), any DNA binding sites present are predicted to be saturated by SDM molecules in the titration as long as SDM is present in excess. Consequently, a graph of the change in SDM absorbance vs the concentration of DNA should be nearly linear until DNA binding sites are in excess, at which point no further significant changes in absorbance should occur. For a macrocycle that obeys the neighbor-exclusion principle, the break point is predicted to be four base pairs per macrocycle, whereas for a macrocycle that violates the neighbor-exclusion principle, a break point of three base pairs per macrocycle is expected (two adjacent sites for binding of the two covalently linked acridines of a macrocycle with neighbor exclusion between bound but not covalently linked acridines). The results obtained for SDM (Figure 3) were more consistent with a three base pair binding site and, consequently, support model iii, binding with violation of the neighbor-exclusion principle.

Dissociation Kinetics. We have found that compounds which have charged side chains in opposite DNA grooves have lower log k_{app} versus log $[Na^+]$ slopes than intercalators with their charged groups in the same groove (Wilson et al., 1990; Tanious et al., 1990). The basis for the difference is the stepwise release of charge interactions for dissociation of opposite groove intercalators and the concerted release of charge interactions for other intercalators. If SDM binds according to model i with both side chains in the same groove, SDM and SPDA would be expected to have similar slopes in log k_{app} versus log $[Na^+]$ plots since they have the same charge. The significantly lower log k_{app} versus log $[Na^+]$ slope for the SDM complex relative to SPDA (Figure 6, supplementary material) is, thus, consistent with model ii or iii for SDM binding with one linking chain in each DNA groove but is not consistent with the bayonet model.

Although models ii and iii predict similar log k_{app} versus log $[Na^+]$ slopes, they also predict a significant difference in DNA association and dissociation rates. Model ii requires simultaneous opening of at least two adjacent base pairs while model iii requires disruption of only one base pair set of hydrogen bonds. Binding of SPDA does not require any base pair hydrogen bonds to be broken. The predicted order of dissociation rate constants would, thus, be largest for the SPDA complex, lower for SDM in a model iii complex, and significantly lower for an SDM model ii complex. SPDA does have the largest dissociation rate constant, which is 10–20 times larger than the SDM rate constants for dissociation from both poly[d(A-T)]$_2$ and poly[d(G-C)]$_2$. This order of dissociation rate constants is as expected for SDM model ii or iii relative to SPDA.

While SDM dissociates from DNA more slowly than the related bisacridine SPDA, it dissociates, at least from poly-[d(G-C)]$_2$, much faster than nogalamycin, which also requires base pair disruption for binding to DNA (Searle et al., 1988; Liaw et al., 1989). Opening of a single base pair to allow exchange of the base pair imino proton with solvent is a demonstrated rapid event, with imino proton half-lives typically on the order of 10–100 ms (Le Roy et al., 1988; Moe & Russu, 1990). Opening of two adjacent base pairs simultaneously should be less probable. One could envision formation of a charge-stabilized preequilibrium groove complex of SDM with DNA that could lead to bisintercalation when two intercalation sites open through thermal motion of the double helix. The acridine rings in such a complex may serve as a surface to catalyze local base pair opening of DNA and facilitate sliding of one linking chain through the double helix. Dissociation would be the reverse of this process. Nogalamycin has only one charge, so that a preequilibrium complex would be much weaker and less probable. In addition, nogalamycin has large substituents on both sides of the intercalator ring system which make partial insertion of the chromophore difficult. Thus, it cannot provide the required surface to catalyze base pair opening as can the two acridines of SDM. It seems quite probable that a macrocyclic bisacridine preequilibrium complex could significantly decrease the activation energy for binding of the macrocycle to DNA, and this can explain the

faster dissociation rate of SDM, relative to nogalamycin, from poly[d(G-C)]$_2$. Another important property of nogalamycin with respect to its kinetic behavior is that it forms two G·C base pair specific hydrogen bonds (Searle et al., 1988; Liaw et al., 1989). These bonds could additionally account for the discrepancy between the rate constants for SDM and nogalamycin dissociation from poly[d(G-C)]$_2$.

NMR. All aromatic protons of SDM in its complex with d(CGCG)$_2$ are shifted upfield in agreement with intercalation models ii and iii. The side-chain protons 1′ and 6′, which are close to the intercalating acridine rings, show positive chemical shifts, indicating that they are also in the positive shielding region above DNA base pairs. Negative chemical shifts are observed for side-chain protons 4′, 5′, 8′, and 9′ which suggests that they are in the negative shielding region at the edges of the DNA base pairs and/or acridine rings. The formation of hydrogen bonds in the complex by the side-chain amide groups could also explain the larger downfield shifts of the 8′ and 9′ protons.

The NMR results place limitations on the possible conformations of SDM in its complex with the CGCG duplex. No cross peaks are observed between the spermine and bisamide side-chain protons at either 25 or 40 °C. The SDM 9′–5 linking chain–acridine ring intramolecular cross peak requires that the bisamide side chain be effectively shortened in that bringing the 9′ side-chain proton into proximity of the aromatic 5 proton reduces the amount of extension possible. Such a conformation can be readily envisioned because it creates an ideal conformation for a hydrogen bond between the protonated nitrogen of the acridine ring and one carbonyl group of the side chain. However, when taken together with the 7′–3 cross peak, the potential for intercalating each acridine into a CG step, according to model ii, is reduced. The negative chemical shift difference for SDM 9′ in the bound vs free states is also consistent with formation of a SDM intramolecular hydrogen bond since the 9′ proton would be located in the region of the acridine/DNA ring current which induces negative shifts.

Substantial evidence supports full intercalation at a CpG step as required by both models ii and iii. The relative magnitudes of the chemical shift differences and the absence of interlinker cross peaks are consistent with the long axis of the acridine ring lying approximately parallel to the long axes of the base pairs (Young & Kallenbach, 1980). The most convincing results, however, are the observed SDM–CGCG cross peaks. The SDM 2 and 3 to C1 2″ cross peaks are in agreement with a full intercalation model for the acridine and cannot be readily reconciled with a bayonet model. The relatively strong SDM 3 to C3 1′ cross peak, which places SDM 3 in the minor groove, is evidence for a model in which the spermine and bisamide side chains are then in the major and minor grooves, respectively. The SDM 1′/6′ to C1 1′/5 cross peak would then be either SDM 1′ to C1 5 or SDM 6′ to C1 1′, with the former more easily modeled in terms of steric constraints. This conclusion is supported by the NOESY spectra at 25 °C (in which the C1 1′ and 5 resonances are resolved) although significant broadening of resonances complicates the assignment.

Accepting one acridine intercalation site as a CpG step, the location of the second acridine binding site is less well-defined. An analysis based on the disappearance of certain duplex connectivities (e.g., G2 2″ to C3 6) upon intercalation of SDM is not feasible due to the combination of the excess of duplex over SDM present and the fast exchange of duplex resonances. A model in which the second acridine end-stacked cannot be completely discounted by the NMR data but is unfavorable from an energetic perspective. Free energy obtained from stacking and electrostatic interactions would be reduced. Experimentally, no G4 2″ cross peaks to SDM aromatic protons are observed as would be expected for such a model. Most convincingly, the chemical shift differences of SDM 2 and 7 in the presence of poly[d(A-T)]$_2$ are similar to those seen in the presence of the CGCG duplex. This result argues for similar binding modes, and end stacking as a mode of binding is not relevant for poly[d(A-T)]$_2$.

The bayonet model (i) predicts a weaker interaction of the macrocycle with DNA than with SPDA since both macrocycle linking chains would have to be crowded into the same groove and only a small part of the acridine rings could stack with DNA base pairs in such a complex. Thus, the bayonet model predicts small visible spectral shifts, lower stability, and faster dissociation kinetics of SDM relative to SPDA complexes. The bayonet model also predicts that the most unobstructed part of the acridine ring (protons 5–8) should be intercalated and should, thus, experience much larger upfield shifts than acridine protons 1–3. Opposite experimental results are obtained in all cases. Additionally, no interchain NOESY cross peaks in the SDM–d(CGCG)$_2$ complex are observed, and the SDM to d(CGCG)$_2$ NOESY cross peaks also do not support a bayonet model. Consequently, on the basis of the current experimental evidence, model i seems unlikely for SDM–polymer complexes and is rejected for the SDM–d(CGCG)$_2$ complex.

The binding of the two acridines at the CpG sites of the CGCG duplex (model ii) can account for many of the observed SDM–CGCG cross peaks. The binding model requires that the two acridines bind asymmetrically with respect to the helical axis; i.e., they are not inverted 180° with respect to each other. Consequently, the two C1 2″ protons are in different environments with one C1 2″ proton proximal to the SDM 2 and 3 side of one acridine ring, and the other near the SDM 6 and 7 side of the second acridine ring. The C1 2′/2″ to SDM 2 and 3 cross peaks would then be associated with the binding site of one acridine ring, and the SDM 6 and 7 to C1 1′/2′/2″ cross peaks would be associated with the binding site of the second acridine. SDM 2 and 3 on the opposite side of the second acridine could then be proximal to C3 2′ and C3 1′, respectively, thereby accounting for those cross peaks. Potential cross peaks which are less definitive—SDM 3 and 8 to the 5′/5″ region and SDM 9′ to G2 1′ or C3 1′—could also be accounted for with the bisintercalation model (These are resolved with stronger weighting functions than the one used for the plot).

While model ii with the acridines intercalated at each of the CG steps would account for many of the observed cross peaks, several cross peaks were observed which would not be predicted by model ii, particularly SDM 2 to G2 2″. An explanation which would account for these cross peaks would be a violation of neighbor exclusion (model iii) in which the middle GC binding site is occupied and either of two binding conformations (SDM 2 and 3 close to C1 2″ or SDM 6 and 7 close to C1 2″) would be possible for the occupied CpG site. Bisintercalative binding in violation of neighbor exclusion would also be consistent with a constrained bisamide side chain as required by the SDM 5 to 9′ and SDM 3 to 7′ cross peaks.

Bisintercalative binding to DNA by certain bisacridine compounds in violation of the neighbor-exclusion principle has been reported previously (Wakelin et al., 1978; Wright et al., 1980; Atwell et al., 1984; Denny et al., 1985), but the binding behavior of some of these compounds has been contested

(Assa-Munt et al., 1985). It is important to note, however, that theoretical studies have shown that intercalation in violation of neighbor exclusion is possible but is disfavored relative to binding by normal intercalation due to a reduction in the release of counterions (Freidman & Manning, 1984). Rao and Kollman (1987) have also shown with molecular mechanics calculations that intercalation of two 9-aminoacridines at adjacent sites (violation of neighbor exclusion) and with an excluded site have very similar energetics.

Although a full molecular modeling study is beyond the scope of this paper, we feel it is important to determine whether stereochemically reasonable complexes of the macrocycle can be built according to models i–iii. Preliminary modeling studies indicate that because of size and steric restrictions, intercalator complexes of the bayonet type (model i) are difficult to dock without severe steric clash, and they have very poor minimized energies relative to the complexes with one chain in each DNA groove. More traditional intercalation complexes according to model ii were relatively easy to dock and gave good interaction energies after minimization. Type iii intercalation complexes were also relatively easy to dock and also produced quite good interaction energies after minimization. At this point in our modeling studies, we can conclude that model i is least likely but cannot definitively distinguish between models ii and iii from the standpoint of molecular mechanics energies.

Consequently, experimental and initial molecular mechanics results both support a model for SDM binding to DNA in which SDM side chains are in opposite grooves. Binding in this manner necessitates temporary disruption of at least one set of Watson–Crick hydrogen bonds during association and dissociation. Moreover, with respect to SDM binding to d-$(CGCG)_2$, the results are, in total, most consistent with bisintercalation in violation of the neighbor-exclusion principle.

Supplementary Material Available

Figure 6, showing plots of log k_{app} versus log [Na^+] for SDM and SPDA binding to DNA (1 page). Ordering information is given on any current masthead page.

Registry No. Poly[d(A-T)], 26966-61-0; poly[d(G-C)], 36786-90-0; d(CGCG), 58927-25-6; SDM, 50815-81-1; SPDA, 58478-35-6.

References

Arnott, S., & Hukins, D. W. H. (1972) *Biochem. Biophys. Res. Commun. 42*, 1504–1507.

Assa-Munt, N., Denny, W. A., Leupin, W., & Kearns, D. R. (1985) *Biochemistry 24*, 1441–1449.

Atwell, G. J., Stewart, G. M., Leupin, W., & Denny, W. A. (1985) *J. Am. Chem. Soc. 107*, 4335–4337.

Besterman, J. M., Elwell, L. P., Cragoe, E. J., Andrews, C. W., & Cory, M. (1989) *J. Biol. Chem. 265*, 2324–2330.

Blackburn, M., & Gait, M. (1990) *Nucleic Acids in Chemistry & Biology*, IRL Press Ltd., Oxford.

Cheng, D. M., Kan, L., Frechet, D., & Ts'o, P. O. P. (1984) *Biopolymers 23*, 775–795.

Crothers, D. M. (1968) *Biopolymers 6*, 575–584.

Delbarre, A., Delepierre, M., Langlois D'Estaintot, M., Igolen, J., & Roques, B. P. (1987) *Biopolymers 26*, 1001–1033.

Denny, W. A., & Wakelin, L. P. G. (1990) *Anti-Cancer Drug Des. 5*, 189–200.

Denny, W. A., Atwell, G. J., Baguley, B. C., & Wakelin, L. P. G. (1985) *J. Med. Chem. 28*, 1568–1574.

Fox, K. R., Brassett, C., & Waring, M. J. (1985) *Biochim. Biophys. Acta 840*, 383–392.

Friedman, R. A. G., & Manning, G. S. (1984) *Biopolymers 23*, 2671–2714.

Gao, X., & Patel, D. (1988) *Biochemistry 27*, 1744–1751.

Gao, X., & Patel, D. J. (1989) *Q. Rev. Biophys. 22*, 93–138.

Hurley, L. H., & Boyd, F. L. (1987) *Annu. Rep. Med. Chem. 22*, 259–268.

Jaycox, G. D., Gribble, G. W., & Hacker, M. P. (1987) *J. Heterocyclic Chem. 24*, 1405–1408.

Laugaa, P., Delepierre, M., Leon, P., Garbay-Jaureguiberry, C., Markovits, J., Le Pecq, J. B., & Roques, B. P. (1987) in *Molecular Mechanisms of Carcinogenic and Antitumor Activity* (Chagas, C., & Pullman, B., Eds.) pp 275–294, Adenine Press, New York.

Le Roy, J. L., Kochoyan, M., Huynh-Dinh, T., & Gueron, M. (1988) *J. Mol. Biol. 200*, 223–238.

Liaw, Y.-C., Gao, Y.-G., Robinson, H., van der Marel, G. A., van Boom, J. H., & Wang, A. H.-J. (1989) *Biochemistry 28*, 9913–9918.

Manning, G. S. (1978) *Q. Rev. Biophys. 11*, 179–246.

Moe, J. G., & Russu, I. M. (1990) *Nucleic Acids Res. 18*, 821–827.

Mohamadi, F., Richards, N. G. J., Guida, W. C., Liskamp, R., Lipton, M., Caufield, C., Chang, G., Hendrickson, T., & Still, W. C. (1990) *J. Comput. Chem. 11*, 440–467.

Muller, W., & Crothers, D. M. (1968) *J. Mol. Biol. 35*, 251–290.

Otting, G., Widmer, H., Wagner, G., & Wuthrich, K. (1986) *J. Magn. Reson. 66*, 187–193.

Pelton, J. G., & Wemmer, D. E. (1990) *J. Am. Chem. Soc. 112*, 1393–1399.

Rao, S. N., & Kollman, P. A. (1987) *Proc. Natl. Acad. Sci. U.S.A. 84*, 5735–5739.

Record, M. T., Anderson, C. F., & Lohman, T. M. (1978) *Q. Rev. Biophys. 11*, 103–178.

Saenger, W. (1984) *Principles of Nucleic Acid Structure* (Cantor, C., Ed.) Springer-Verlag, New York.

Scott, E. V., Zon, G., Marzilli, L. G., & Wilson, W. D. (1988) *Biochemistry 27*, 7940–7951.

Searle, M. S., Hall, J. G., Denny, W. A., & Wakelin, L. P. G. (1988) *Biochemisty 27*, 4340–4349.

States, D. J., Haberkorn, R. A., & Ruben, D. J. (1982) *J. Magn. Reson. 48*, 286–292.

Strickland, J. A., Marzilli, L. G., Gay, K. M., & Wilson, W. D. (1988) *Biochemistry 27*, 8870–8878.

Suzuki, M. (1990) *Nature 344*, 562–565.

Tanious, F., Yen, S.-F., & Wilson, W. D. (1990) *Biochemistry* (submitted for publication).

Wakelin, L. P. G. (1986) *Med. Res. Rev. 6*, 275–340.

Wakelin, L. P. G., Atwell, G. J., Rewcastle, G. W., & Denny, W. A. (1987) *J. Med. Chem. 30*, 855–861.

Wakelin, L. P. G., Romanos, M., Chen, T. K., Glaubiger, D., Cannellakis, E. S., & Waring, M. J. (1978) *Biochemistry 17*, 5057–5063.

Warshaw, M., & Cantor, C. (1970) *Biopolymers 9*, 1079–1103.

Weiner, S. J., Kollman, P. A., Nguyen, D. T., & Case, D. A. (1986) *J. Comput. Chem. 7*, 230–252.

Wells, R. D., & Harvey, S. C. (1987) *Unusual DNA Structures*, Springer, New York.

Wilson, W. D. (1990) in *Nucleic Acids in Chemistry & Biology* (Blackburn, M., & Gait, M., Eds.) Chapter 8, IRL Press Ltd., Oxford.

Wilson, W. D., & Li, Y. (1991) NMR Analysis of Reversible Nucleic Acid–Small Molecule Complexes. In *Advances in DNA Sequence Specific Agents* (Hurley, L., Ed.) JAI Press, London (in press).

Wilson, W. D., Krishnamoorthy, C. R., Wang, Y.-H., & Smith, J. C. (1985) *Biopolymers 24*, 1941–1961.
Wilson, W. D., Dotrong, M. H., Zuo, E. T., & Zon, G. (1988) *Nucleic Acids Res. 16*, 5137–5155.
Wilson, W. D., Tanious, F. A., Buczak, H., Venkatramanan, M. K., Das, B. P., & Boykin, D. W. (1990) in *Molecular Basis of Specificity in Nucleic Acid–Drug Interactions, The 23rd Jerusalem Symposium on Quantum Chemistry and Biochemistry* (Jortner, J., & Pullman, B., Eds.) Reidel, Dordrecht, Holland (in press).
Wright, R. G. M., Wakelin, L. P. G., Fieldes, A., Waring, M. J., & Acheson, M. (1980) *Biochemistry 19*, 5825–5836.
Wuthrich, K. (1986) *NMR of Proteins and Nucleic Acids*, John Wiley & Sons, New York.
Young, P. R., & Kallenbach, N. R. (1980) *Proc. Natl. Acad. Sci. U.S.A. 11*, 6453–6457.
Zimmerman, S. C., Lamberson, C. R., Cory, M., & Fairley, T. A. (1989) *J. Am. Chem. Soc. 111*, 6805–6809.

Asymmetric Structure of a Three-Arm DNA Junction†

Qiu Guo,‡ Min Lu,‡ M. E. A. Churchill,§ T. D. Tullius,§ and N. R. Kallenbach*,‡
Department of Chemistry, New York University, New York, New York 10003, and Department of Chemistry, The Johns Hopkins University, Baltimore, Maryland 21218
Received July 18, 1990; Revised Manuscript Received September 5, 1990

ABSTRACT: We present here experimental evidence that three-arm branched DNA molecules form an asymmetric structure in the presence of Mg^{2+}. Electrophoretic mobility and chemical and enzymatic footprinting experiments on a three-arm branched DNA molecule formed from three 16-mer strands are described. The electrophoretic mobilities of three species of a three-arm junction in which pairs of arms are extended are found to differ in the presence of Mg^{2+}: one combination of elongated arms migrates significantly faster than the other two. This effect is eliminated in the absence of Mg^{2+}, leading us to suggest that the three-arm DNA junction forms an asymmetric structure due to preferential stacking of two of the arms at the junction in the presence of Mg^{2+}. The pattern of self-protection of each 16-mer strand of the core complex exposed to Fe(II)·EDTA and DNase I scission is unique, consistent with formation of an asymmetric structure in the presence of Mg^{2+}. We conclude that three-arm junctions resemble four-arm junctions in showing preferential stacking effects at the branch site. Comparison of the scission patterns of linear duplexes and the branched trimer by the reactive probes methidiumpropyl-EDTA·Fe(II) [MPE·Fe(II)] and Cu(I)–[*o*-phenanthroline]$_2$ [$(OP)_2Cu^I$] further indicates that the branch point represents a site of enhanced binding for drugs, as it does in the four-arm case. Reaction with diethyl pyrocarbonate (DEPC), a purine-specific probe sensitive to conformation, is enhanced at the branch site, consistent with loosening of base pairing or unpairing at this point. The resolving enzyme, bacteriophage T7 endonuclease I, cleaves each of the three stands of the three-arm junction one nucleotide away from the branch with roughly equal efficiency. Thus while the structure of the three-arm junction appears to reflect preferential stacking of particular arms in the presence of Mg^{2+}, it differs in fundamental respects at the branch from that observed in four-arm structures.

There is growing interest in the biological and physical properties of variant states and structures of DNA that are functionally relevant, including sites of base mismatches (Hunter et al., 1986), bulges (Williams & Goldberg, 1988a,b), bends of the helix axis (Hagerman, 1986; Koo et al., 1986), cruciforms (Mizuuchi et al., 1982), and other branched species (Seeman et al., 1989), as well as H-DNA (Htun & Dahlberg, 1988). Certain states of DNA, such as Holliday branched recombination junctions (Holliday, 1964), are stable only transiently; it is necessary to trap these intermediates in order to avoid resolution of the system into two duplexes by the process of branch migration (Kim et al., 1972; Meselson & Radding, 1975; Warner et al., 1978). By selecting symmetry-breaking sequences that are thermodynamically stable, the branch point in a four-arm model Holliday intermediate can be fully or partially immobilized, providing a general system of stable oligonucleotide models for recombination intermediates (Seeman et al., 1989). Much work on this system has focused on the four-arm junction, which allows one to investigate properties of Holliday-type intermediates (Kallenbach & Seeman, 1986; Cooper & Hagerman, 1987, 1989; Duckett et al., 1988). Since three-arm intermediates can also arise as intermediates in general recombination in the absence of replication (Broker & Doermann, 1975; Minagawa et al., 1983; Jensch & Kemper, 1986), there is reason to investigate the structural and substrate properties (Jensch & Kemper, 1986; Dickie et al., 1987) of these species as well.

Gel electrophoresis has been widely used to investigate the properties of stable DNA junctions (Cooper & Hagerman, 1987; Duckett et al., 1988; Seeman et al., 1989). Cooper and Hagerman (1987) studied a four-arm synthetic junction by gel electrophoresis under native conditions, utilizing the fact that bent DNA molecules have reduced mobilities on polyacrylamide gels to an extent that varies with the apparent degree of the bend angle (Koo et al., 1986). Cooper and Hagerman (1987) formed a set of molecules in which long duplex arms were appended pairwise to a four-arm complex

† This research was supported by Grants CA-24101, GM-40894, and CA-01208 from the National Institutes of Health; T.D.T. has received an NIH Research Career Development Award, an Alfred P. Sloan Fellowship, and a Camille and Henry Dreyfus Teacher–Scholar Award.
* Author to whom correspondence should be addressed.
‡ New York University.
§ The Johns Hopkins University.

0006-2960/90/0429-10927$02.50/0 © 1990 American Chemical Society